PREDICTION OF CONVECTIVE HEAT TRANSFER COEFFICIENTS AND EXAMINATION OF THEIR EFFECTS ON DISTORTION OF CYLINDRICAL TUBES QUENCHED BY GAS COOLING

A. Thuvander, A. Melander, M. Lind, N. Lior, F. Bark

The primary objectives of this study are to model the nature of the high-turbulence complex quenching cooling-gas flow, with flow separations, and to examine its effects on the resulting distortions, here of bearing steel tubes. A k–∈ turbulent flow and heat transfer model we have adopted was found to predict the convective heat transfer coefficient distribution reasonably well for Reynolds number up to about (0.3) 10⁶. At higher Reynolds number (here examined up to 10⁶) it predicts them reasonably well in most of the cylinder windward and leeward zones, and predicts well the angles at which transition to turbulent starts and at which the flow separates, as well as the existence of two maxima and two mininia in the heat transfer coefficient. It, however predicts values about 100% higher than those available from the available experimental data in the laminar-to-turbulent boundary layer transition zone. This model, as well as available experimental and representative data, were used to define the distributions of the convective heat transfer coefficient around the body surface as the boundary condition of a finite-element program developed at the Swedish Institute for Metals Research for predicting the temperature distribution history, phase transformations, distortions and mechanical properties of quenched steel bodies. The dependence of the distortions on the extent of convective heat transfer coefficient nonuniformity was analyzed.

INTRODUCTION

Environmental problems associated with the use of oils and other liquids in the quenching of steel have been one of the primary motivators for the increased interest in their replacement by inert gases, such as nitrogen, helium and hydrogen [1]. To obtain convective heat transfer coefficients (h) that are high enough for gas quenching it is necessary to use high gas velocities, which unfortunately result in severe variations of these coefficients along the quenched surface. These variations cause nonuniformities in the temperature distribution in the quenched body, with consequently undesirable distortions, residual stresses, and nonuniformities in its mechanical properties (cf. [2]-[7]).

Anders Thuvander and Arne Melander,
Swedish Institute for Metals Research, Stockholm, Sweden

Mats Lind, Fritz Bark,
Faxén Laboratoriet, Stockholm, Sweden

Noam Lior, *Dept. of Mech. Engng & Appl. Mech. University of Pennsylvania, Philadelphia, U.S.A.*

Memoria presentata al 11th Conference of the International Federation for Heat Treatment and Surface Engineering - 4th ASM Heat Treatment and Surface Engineering Conference in Europe

To illustrate the problem, Fig. 1 demonstrates the flow, heat transfer and nonuniformities as computed by the Faxén laboratory team for the conjugate convective-conductive problem [8] for cross-flow quenching of a steel cylinder initially at 1200 K, by means of nitrogen at 10 bar 300 K, with Reynolds number Re = (3.16) 10^5, Prandtl number Pr = 0.7, Biot number Bi = 0.66, at Fourier number Fo = 0.13. The boundary layer thickens from the stagnation point downstream until separation is seen to occur at about 100°, followed by a recirculation zone and wake. h is seen to be, as expected, high in the stagnation region, gradually decreasing downstream as the boundary layer thickens, rising to a rnaximum in the flow separation region, then decreasing, and further downstream slightly increasing in the wake region. A k–∈ turbulent flow and heat transfer model was adapted which predicts the h distribution over cylinders much better than two of the most popular ones in use, but still has local errors of up to 40%. One of the conclusions was that the magnitude of the maximal temperature gradient in the quenched body is highly sensitive to the local magnitude of h.

The primary objective of this study is to exarnine the effects of the nature of the cooling gas flow on the distortions in metals during quenching. To that end we

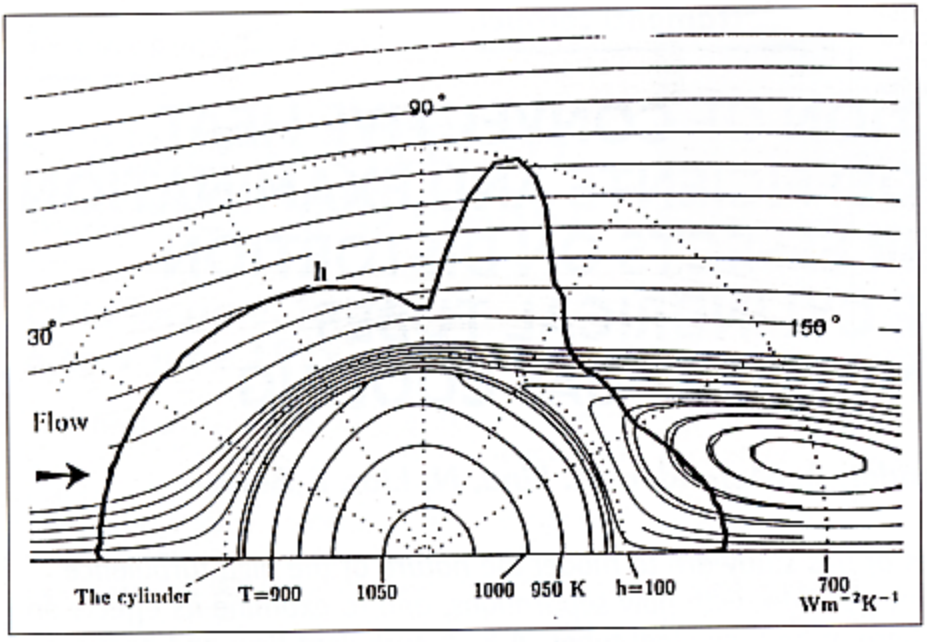

Fig. 1 - Typical streamlines, surface convective heat transfer coefficient (h), and internal temperature (T) distribution as computed [8] for the crossflow quenching of a stainless steel cylinder.
Initial cylinder temperature = 1200 K
gas temperature = 300 K
thermal conductivity of the steel = 20 $Wm^{-1}K^{-1}$,
Re = (0.316) 10^6,
Prandtl number = 0.7,
Biot number = 0.66,
Fourier number = 0.27.

Fig. 1 - Linee di flusso tipiche del coefficiente di trasferimento di calore convettivo (h) e distribuzione della temperatura interna (T) secondo l'elaborazione [8] per la tempra di un cilindro di acciaio inossidabile.

have computed the turbulent flow convective heat transfer coefficients along the circumference of a tube for Reynolds numbers of (0.316)10^6, (0.491)10^6, and 10^6 compared them to some available experimental data, and computed the distortions in the ring due to the nonuniformities in these heat transfer coefficients.

FLOW MODELING AND THE CONVECTIVE HEAT TRANSFER COEFFICIENTS

Background

To obtain the high heat transfer coefficients needed for quenching, high gas velocities and pressures are needed, resulting in flow Reynolds numbers of 10^5 - 10^7. The flow is thus highly turbulent, and furthermore goes through separation and formation of complex wake-type regions. In an effort to identify a reasonable way for predicting the distribution of h along the body surface, the Faxén Laboratory team as focused [8] on several variants of the k–ϵ model, which is currently probably still the only practical model for solving turbulent flow problems in realistic applications. At the same time, while these models often account reasonably well for some of the overall flow parameters such as the pressure coefficient, they and others have found that they typically produce large errors in the prediction of the h distribution.

The numerical analysis in [8] and in this study was performed by using the commercial finite-difference code CFX [9].

A low free-stream turbulenee of 1.2% was chosen. It was found in [8] that the Launder and Sharma [10] κ–ε model as modified by Yap [11] and Cho and Goldstein [12] with particular concern for recirculating flows, was overah the best o f the models for the Re=(0,316)10^6 considered, but that it stile has errors of up to about 40% in h, underpredicting it to that extent in the separated flow region. Since this was the most suitable model they have found or developed so far, wc have used it also in this study.

The numerical predictions of the h distributions was performed for three Reynolds numbers: (0.316)10^6, (0.491)10^6, and 10^6, chosen because they are in the range relevant for gas-cooled heat treatment and because experimental data (from [13]) was available for comparison. The results of the numerical prediction of the h value

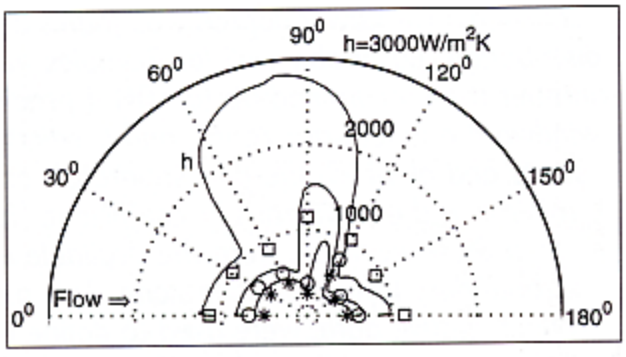

Fig. 2 - Convective heat transfer coefficient (h) distributions for air flow across a cylinder, as predicted from the numerical analysis (solid lines) and from the experimental data of [13]. Re = (0.316)10^6 (*); (0.491) 10^6; (o) = 10^6 (❑).

Fig. 2 - Distribuzioni del coefficiente di trasferimento di calore convettivo (h) per flusso d'aria attraverso un cilindro, in accordo con le predizioni dell'analisi numerica (linee continue) e con i dati sperimentali di [13]. Re = (0.316)10^6 (*); (0.491) 10^6; (o) = 10^6 (❑).

distributions, alongside with experimental values from the literature 1 3 are shown in Fig. 2.

The Flow and its Relation to the Convective Heat Transfer Rates

Generally, the variations of the convective heat transfer coefficient along the cylinder circumference (h) may be attributed to the level of turbulence in the boundary layer, and to the boundary layer thickness. The nature of the variations, as observed in Fig. 2, is singular for all of the Reynolds numbers considered here. Examining the flow as shown in Fig. 1 and Fig. 3a, starting from the forward stagnation point and moving along the cylinder surface from windward to leeward, there is first a laminar boundary layer which becomes gradual thicker, with a corresponding decrease in h. When the boundary layer starts becoming turbulent, in transition where h reaches its first minimum, the change from the laminar behavior results in an increase in h, up to a maximum where the boundary layer becomes fully turbulent. As the fully turbulent boundary layer then gradually thickens, the rate of increase of h starts slowing down, reaching the maximum of h at the separation point (Fig. 3b), where it then drops rapidly to its second minimum. On the leeward

Fig. 3 - Velocity and h distributions for Re=10^6.
a. The entire flow.
b. Detail at separation.
c. Detail at leeward surface (note the reverse flow).

Fig. 3 - Distribuzioni di h e velocità per Re=10^6.
a. L'intero flusso.
b. Dettaglio alla separazione.
c. Dettaglio presso la superficie sottovento (notare il flusso inverso).

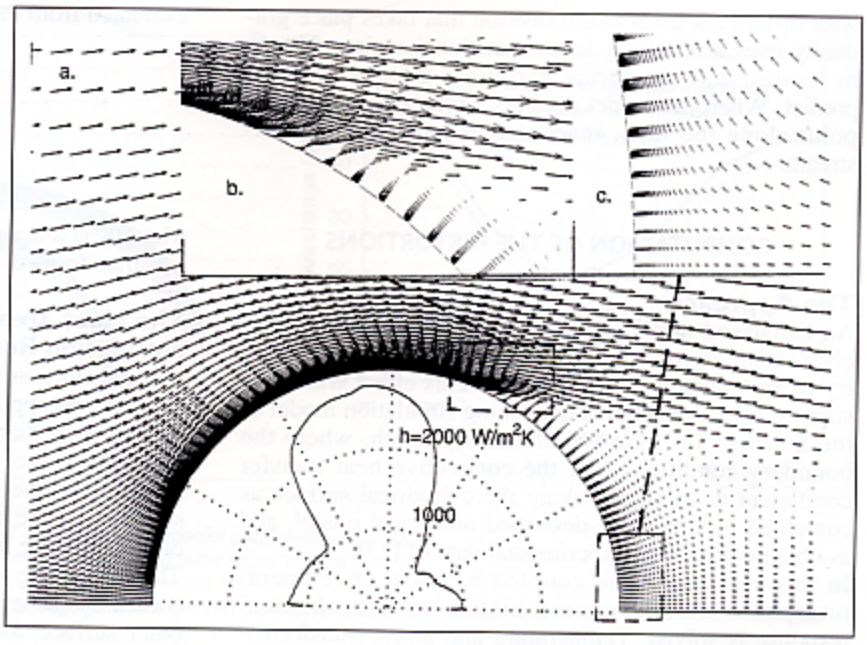

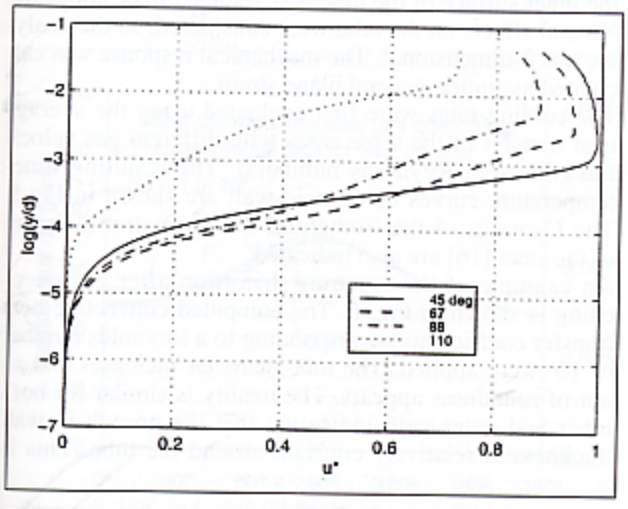

Fig. 4 - Boundary layer velocity profiles at several azimuthal angles along the cylinder surface. y/d: dimensionless coordinate normal to the cylinder of diameter d. u*: azimuthal velocity normalized by the free stream velocity.

Fig. 4 - Profili della velocità allo strato del bordo a diversi angoli di azimut lungo la superficie del cilindro. y/d = normale coordinata senza dimensioni per il cilindro di diametro d. u*: velocità all'azimut normalizzata dalla velocità del libero flusso.

part of the cylinder, the flow direction is reversed (Fig. 3c), and a turbulent boundary layer starts developing from the rear stagnation point, where h attains its second maximum. h gradually decreases as this boundary layer thickens, from the rear stagnation point to the separation point.

To better understand the boundary layer transitions, which can not be discerned from Fig. 3, boundary layer velocity profiles at 4 angles are shown in Fig. 4. For example, the boundary layer thickens by approximately 1.5 orders of magnitude from the angle of 45° to 110°. Coincidentally the velocity outside the boundary layer diminishes as the flow changes from an accelerating one on the windward side of the cylinder to a decelerating one at the lee side. The near-wall slope of the velocity profiles allows the distinction of laminar form turbulent flows: for the smaller angles the velocity profiles have smooth slope transitions, characteristic of laminar flow, which gradually show more abrupt slope transitions and near-linear shape as the boundary layer becomes turbulent (where the logarithmic wall law is employed).

Comparison between the Numerical and Experimental Results

Figure 2 shows that the adaption of the k–∈ Launder-Sharma - Yap - Cho-Goldstein model at Re = (0.316)10^6 was able to reduce the difference between the numerically-predicted and experimental convective heat transfer coefficients to 40% at most [8]. It also shows that at the higher values of Re the numerical results appear to over-predict these coefficients by about 100% at worst, in the transition and turbulent boundary layer regimes. The errors are smaller at the upstream surface of the cylinder where the boundary layer is laminar, and on the downstream surface between the separation and downstream stagnation points. Notably, the angle at which boundary layer transition commences, and at which the flow separates, are predicted by the model reasonably well, and thus the model also predicts the locations of the maxima and minima of h reasonably well.

It is useful to understand the discrepancies between the experimental and numerical predictions, primarily so that the modeling can be effectively improved (an ongoing effort at the Faxén Laboratory). We first note that although the experimental data of [13] are widely used in the literature, we are not aware of any corroboration by other research groups, and thus we can not regard them as the correct basis for comparison. We are also in the process of starting some experimental work and expect to clarify this issue. Secondly, the turbulent flow and heat transfer models used in this work were developed for high Reynolds numbers, with a low-Reynolds number extension to handle the boundary layer near the wall. The low-Re extension was developed for flow over a fiat plate or a channel wall. This is different from the situation here, where pressure gradients are affecting the boundary layer, and where the boundary layer develops over a curved surface.

Since the largest differences occur at the region of transition from laminar to turbulent flow, we note that the numerical modelling there is indeed based on the weakest- assumptions. One of the weaknesses is that these models do not take into account the experimentally-observed fact that the boundary layer is intermittent, i.e. switching irregularly in and out of the turbulent regime

with time. This leads to a transition that takes place gradually over a relatively long transitional region. This is m contrast with the abrupt transitions that such models predict. When the model predicts wrong results at some point along the flow, inaccuracies are carried downstream.

COMPUTAT'ION OF THE DISTORTIONS

The Approach

As discussed above, quenching of an axi-symmetric object with asymmetric cooling is likely to destroy the s try by out-of-roundness distortion. This effect was investigated here by using the quenching simulation model of the Swedish Institute for Metals Research, where the boundary condition were the convective heat transfer coefficient distributions along the cylindrical surface as computed by the above-described numerical model, and as obtained from the experimental data of [13].
In this simulation the coupled problem of temperature/phase transformation history and mechanical response is solved. Temperature and phase transformations are evaluated in a separate simulation and the results are introduced in the subsequent simulation of the mechanical response.

The Distortion Simulation Model

The simulation quenching simulation model is based on the finite element method using a combination of a commercial FEM-code AB AQUS [14] and own software [6, 7]. Latent heat from phase transformation is modeled as an internal heat source with the volume heat flux proportional to the rate of transformation. The amount of phase transformed is evaluated using generalized Kolrnogorov - Johnson-Mehl - Avrami (KJMA) expressions for diffusion controlled transformations, and the Kolstinen-Marburger equation [15] for martensite transformation.
In the simulation of the mechanical response the plastic flow is described with the following pair of equations that are integrated numerically.

$$\dot{\varepsilon}^{eq} = \dot{\varepsilon}_0 \left(\frac{\sigma}{\sigma_0} \right)^n r^{-m}, \qquad (1)$$

$$\dot{r} = \dot{\varepsilon}^{eq} - Cr^2. \qquad (2)$$

Equation (1) is a creep equation here given for uniaxial tension. It gives the rate of equivalent plastic strain as a function of the equivalent von Mises stress σ and the variable r which can be regarded as a normalised dislocation density $r = \rho/\rho_0$. As an initial condition it is set to zero. The equations include the temperature dependent material constants σ_0, n, m and C while $\dot{\varepsilon}_0$ is a fixed strain rate. Equation (2) describes recovery of dislocation density and accordingly the strain hardening. The parameter C in this equation is strongly temperature dependent. At low temperatures C is close to zero and r becomes almost equal to the plastic strain. The tensor of plastic strain ε^{pl}_{ij} can be evaluated from the stress deviation tensor S_{ij}, the equivalent stress and the rate of equivalent plastic strain from eq. (1) by

$$\dot{\varepsilon}^{pl}_{ij} = \frac{3}{2\sigma} S_{ij} \dot{\varepsilon}^{eq}. \qquad (3)$$

An additional contribution to the plastic strain is assumed to be due to the micro mechanical effect of transformation plasticity. The strain from this mechanism, ε^{tp}_{ij}, is evaluated from the following equation

$$\dot{\varepsilon}^{tp}_{ij} = \frac{3}{2} K S_{ij} g'(f) \dot{f}$$
$$g'(f) = 2(1 - f), \qquad (4)$$

where K is a material parameter and f is the volume fraction transformed.

The Heat Treatment Distortion Simulation Results

In the distortion simulation it was assumed that the heat transfer was applied to the outer surface of a long tube of 32 mm outer diameter and 1.5 mm wall thickness. These dimensions were selected to obtain a cooling rate, corresponding to the gas-quenching flow Reynolds numbers selected for the analysis, that is sufficient for producing only martensite transformation of this steel.
The tubes were assumed to be austenitized at 860°C and cooled by gas at 20°C. Cooling was only applied on the outer surface, as described in the previous section, and the inner surface of the tube was assumed to be adiabatic. No end effects on the tube were considered, so the analysis was 2-dimensional. The mechanical response was calculated assuming general plane strain.
The cooling rates were first evaluated using the average heat transfer of the three cases with different gas velocities (different Reynolds numbers). The resulting time-temperature curves of the mid-wall are shown in Fig.5. The C-curves of the isothermal transformation diagram of the steel [16] are also indicated.
An example of the resulting distortion after gas quenching is shown in Fig. 6. The computed convective heat transfer coefficients corresponding to a Reynolds number of 10^6 were applied. The tube diameter increases and an out-of-roundness appears. The ovality is similar for both inner and outer radii indicating that the growth in wall thickness is relatively constant around the tube. This is

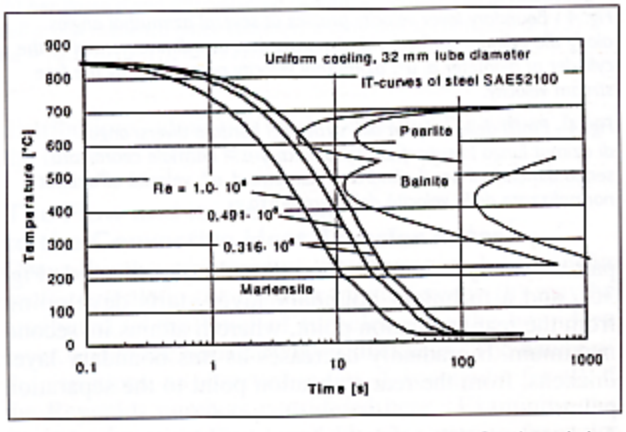

Fig. 5 - Calculated time-temperature at mid-wall for uniformly cooled tubes of 32 mm outer diameter and 1.5 mm wall thickness. The constant heat transfer coefficients used are averages of the experimental values for the different Reynolds numbers: Re = (0.316)10⁶; h = 430 W/(M² K); Re = (0. 491)10⁶; h = 575 W/(M² K); Re =10⁶; h = 1026 W/(M² K). Isothermal transformation curves of 1% and 99% transformation and Ms are overlaid.

Fig. 5 - Tempo-temperatura calcolato a metà parete di tubi del diametro esterno di 32 mm e spessore di 1,5 mm raffreddati uniformemente. I coefficienti costanti del trasferimento di calore usati sono una media dei valori sperimentali per i numeri Reynolds: Re = (0.316)10⁶; h = 430 W/(M² K); Re = (0. 491)10⁶; h = 575 W/(M² K); Re =10⁶; h = 1026 W/(M² K). Le curve di trasformazione isotermica 1% e 99% e Ms sono sovrapposte.

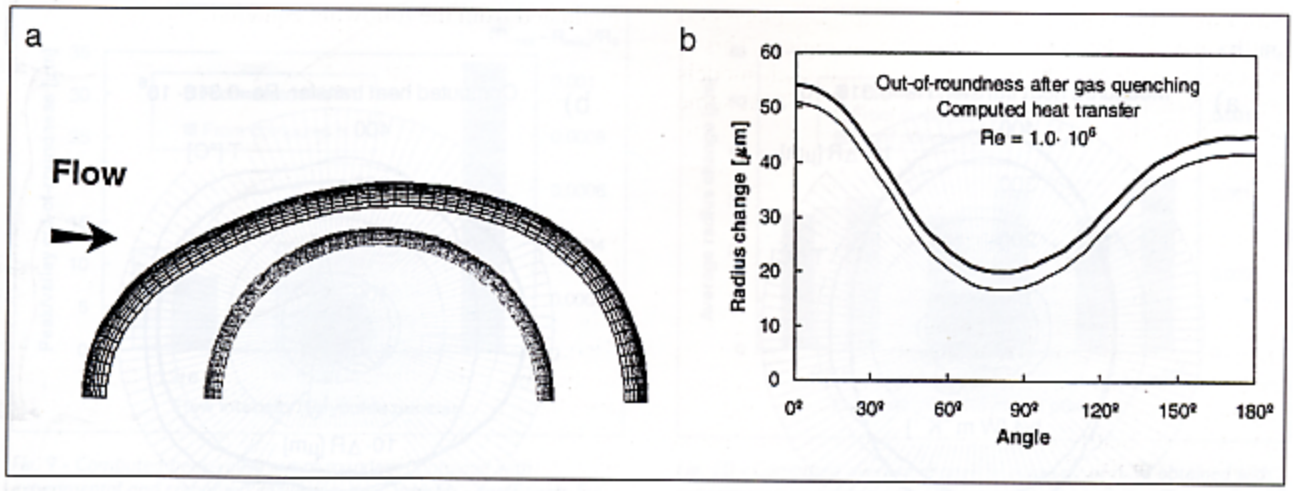

Fig. 6 - Computed distortion of tubes after gas quenching.
The computation was performed with the computed convective heat transfer coefficients at Re 10⁶.
a) Deformed mesh (displacements magnified 200 times). b) Inner and outer radius change

Fig. 6 - Distorsione elaborata sul raggio esterno di tubi dopo tempra a gas con tre diverse velocità di flusso corrispondenti a diversi numeri Reynolds.
a) Simulazione con h sperimentale.
b) Simulazione con h elaborata.

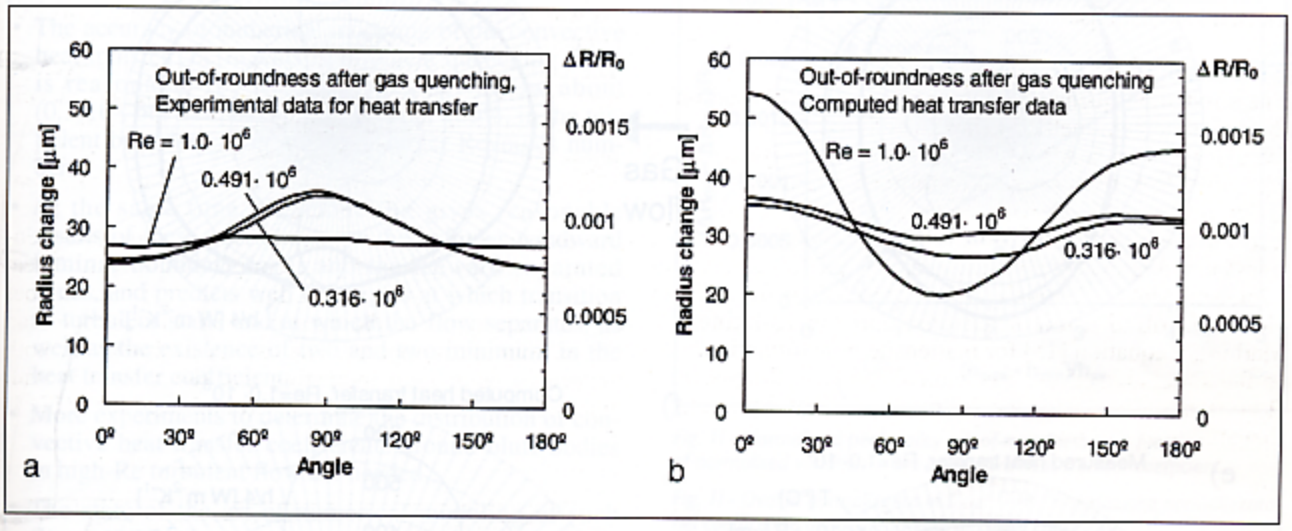

Fig. 7 - Computed distortion on outer radius of tubes after gas quenching with three different flow rates corresponding to different Reynolds numbers.
a) Simulation with experimental h. b) Simulation with the computed h.

Fig. 7 - Distorsione elaborata sul raggio esterno di tubi dopo tempra a gas con tre diverse velocità di flusso corrispondenti a diversi numeri Reynolds.
a) Simulazione con h sperimentale. b) Simulazione con h elaborata.

true for all the tubes considered here, because they are thin, and in Fig. 7 only the distortion of the outer radius is shown.

The distortion obtained by using the experimentally-obtained convective heat transfer coefficients shows a somewhat different ou-of-roundness than obtained with the computed ones. In the former case the tube radius grows the most at an angle of 90° to the gas flow. In the latter case the largest radius growth generally appears parallel to the gas flow.

In both cases the nature and magnitude of the distortions changes with the cooling flow Reynolds number. With the experimental heat transfer data the highest Reynolds number gives less out-of-roundness than for the lower gas flow and Re. With calculated heat transfer data the highest Re gives worst out-of- roundness. A clear relationship between the distributions of the convective heat transfer coefficients, the surface temperature and the outer radius change (distortion) is shown in Fig. 8.

The calculated peak to valley out-of-roundness, Fig. 9 is evaluated as the largest radius minus the smallest radius of the quenched tube.

Although the orientation of the ovality is different for measured and computed heat transfer, the order-of-magnitude of the distortion is similar for the small Reynolds numbers. For higher cooling rates the differences are significantly larger. The average radius growth, Fig. 10, is generally somewhat larger for non-uniform cooling than for uniform cooling using the average heat transfer coefficient.

It is clear that increasing variations in heat transfer coefficients around a circular object will increase the probability of large out-of-roundness. A simple measure of this variation is the difference between the largest and the smallest heat transfer coefficient around the tube divided by the average heat transfer coefficient. The normalized peak-to-valley out-of-roundness is given as a function of this number in Fig. 11.

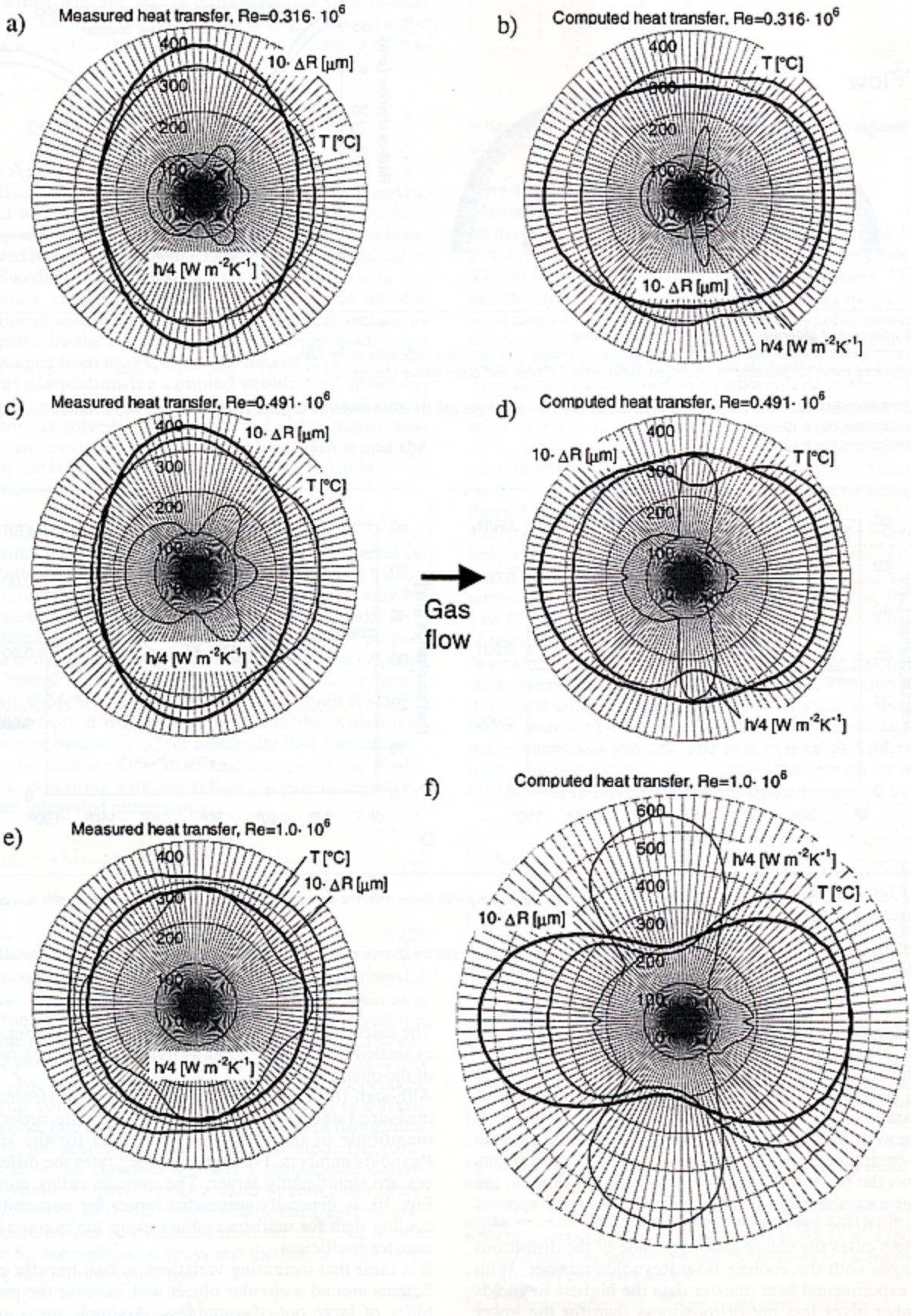

Fig. 8 - Polar diagrams of the convective heat transfer coefficients h, surface temperature T and outer radius change ΔR during quenching. The temperature is given after 20 s cooling for Re=(0.316)10⁶, after 14 s for Re=(0.491)10⁶ and after 7 s for Re= 10⁶.

Fig. 8 - Diagrammi polari dei coefficienti del trasferimento di calore convettivo h, temperatura superficiale T e variazioni del raggio esterno ΔR durante tempra. La temperatura è riportata per il raffreddamento dopo 20 s per Re=(0.316)10⁶, dopo 14 s per Re=(0.491)10⁶ e dopo 7 s per Re= 10⁶.

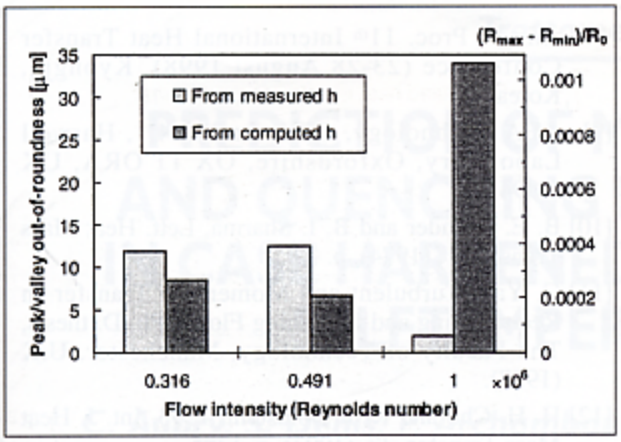

Fig. 9 - Computed peak-valley out of-roundness obtained with experimental and computed convective heat transfer - coefficients for different Reynolds numbers.

Fig. 9 - Istogramma elaborato per l'ovalità ottenuta con i coefficienti del trasferimento di calore convettivo sperimentali e calcolati per i diversi numeri di Reynolds.

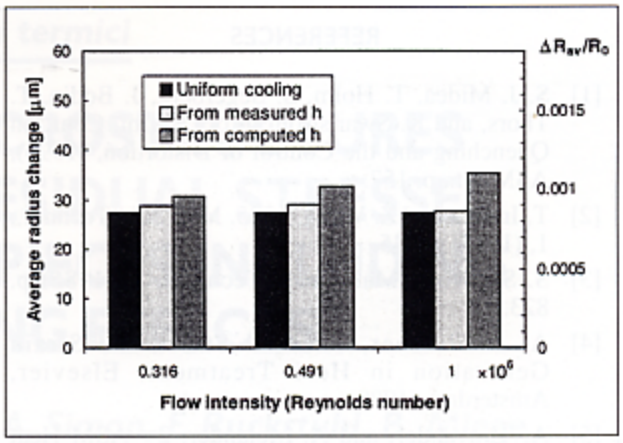

Fig. 10 - Computed average change in diameter of rings obtained with experimental and computed convective heat transfer coefficients for different Reynolds numbers.

Fig. 10 - Cambiamento medio calcolato nel diametro di anelli ottenuti con coefficienti del trasferimento di calore convettivo per i diversi numeri di Reynolds.

CONCLUSIONS AND RECOMMENDATIONS

- The accuracy of numerical modeling of the convective heat transfer coefficients in turbulent quenching flows is reasonable for Reynolds number below about $(0.3)10^6$, but has peak errors of about 100%, in the turbulent boundary layer zone, for larger Reynolds numbers.
- At the same time, the modeling gives reasonable results of these coefficients on the cylinder windward laminar boundary layer and the leeward separated zones, and predicts well the angles at which transition to turbulent starts and at which the flow separates, as well as the existence of two and two minimum in the heat transfer coefficient.
- More experiments to determine the distribution of convective heat transfer coefficients around bluff bodies in high-Re turbulent flow are needed.
- The state of the art of numerical modeling of such flows must be improved.
- Increasing variation in the convective heat transfer coefficient around a circular object clearly increase the probability of large out-of-roundness
- The distortion obtained by using the experimentally-obtained convective heat transfer coefficients shows a somewhat different out-of-roundness than obtained with the computed ones. In the former case the tube radius grows the most at an angle of 90° to the gas flow. In the latter case the largest radius growth generally appears parallel to the gas flow.
- The average radius growth is generally somewhat larger for non-uniform cooling than for uniform cooling using the average heat transfer coefficient.

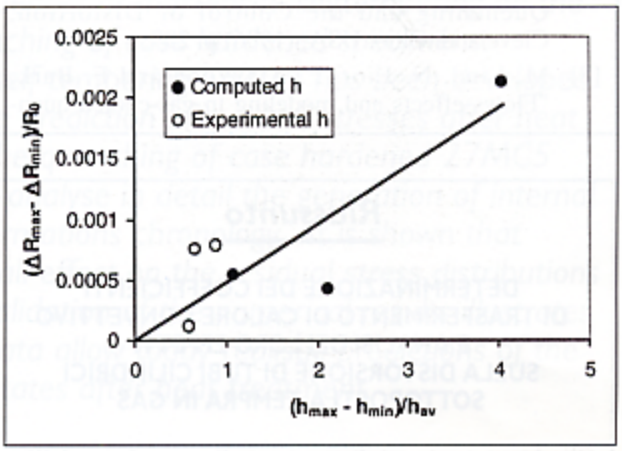

Fig. 11 - Normalized peak-valley out-of-roundness as a function of normalised variation in the convective heat transfer coefficient.

Fig. 11 - Ovalità normalizzata in funzione della variazione normalizzata nel coefficiente del trasferimento di calore convettivo.

ACKNOWLEDGMENT

This work at the Faxén Laboratory of the Royal Institute of Technology, Stockholm was supported by AGA AB, SKF, and Volvo. The distortion calculations were performed at the Swedish Institute for Metals Research, financed by its General Research Programme.

REFERENCES

[1] S. J. Midea, T. Holm, S. Segerberg, J. Bodin, T. Thors, and K. Swartstrom, Proc. 2nd Int. Conf. on Quenching and the Control of Distortion, (1996), ASM Int., p. 157.

[2] T. Inolm, and Z. Wang, 1985. Mat. Sci. Technol., 1, (1985) p. 845.

[3] S. Sjöström, Mat. Sci. &Technol., 1, (1985) p. 823.

[4] A. J. Fletcher, Thermal Stress and Strain Generation in Heat Treatment, Elsevier, Amsterdam (1989).

[5] A. Thuvander, and A. Melander, 2nd ASM Heat Treatment and Engineering Conference, Dortmund, Germany (1993), 2, p. 641.

[6] A. Thuvander, Numerical simulation of distortion due to heat treatment, Licentiate thesis, Report KTH/AMT-143, Royal Institute of Technology, Stockholm Sweden (1995).

[7] A. Thuvander 1996, Proc. Second Int. Conf. on Quenching and the Control of Distortion, Cleveland, Ohio, USA, (1996) p. 297.

[8] M. Lind, N. Lior, F. Alavyoon and F. Bark, "Flows effects and modeling in gas-cooled quenching", Proc. 11th International Heat Transfer Conference (23-28 August 1998), Kyongju, Korea.

[9] AEA Technology, CFX version 4.1, Harwell Laboratory, Oxfordshire, OX 11 ORA, UK (1994).

[10] B. E. Launder and B. I. Sharma, Lett. Heat Mass Transfer, 1, (1974), p. 131.

[11] C. Yap, Turbulent and Momentum Transfer In Recirculating and Impinging Flows. Ph. D. thesis, The Faculty of Technology, Manchester, U.K (1987).

[12] H. H. Cho and R. J. Goldstein, 1993. Int. J. Heat Mass Transfer, 37, (1993), p. 1795.

[13] A. Zukauskas, and J. Ziugzda, Heat Transfer of a Cylinder in Crossflow, Hemisphere, Washington, DC (1984).

[14] ABAQUS Users Manual to version 5.7, Hibbit, Karlsson and Sorensen Ine., Pawtucket, Rhode Island (1997).

[15] D. P. Koistinen and R. E. Marburger, Aeta Metallurgica, 7 (1959), p. 50.

[16] SKF, The Black Book, SKF Steel, Sweden (1984).

Riassunto

DETERMINAZIONE DEI COEFFICIENTI DI TRASFERIMENTO DI CALORE CONVETTIVO E ANALISI DEI LORO EFFETTI SULLA DISTORSIONE DI TUBI CILINDRICI SOTTOPOSTI A TEMPRA IN GAS

Gli obiettivi primari di questo studio sono la modellizzazione della natura del complesso flusso del gas di tempra ad alta turbolenza, con separazioni del flusso, nonché l'analisi dei suoi effetti sulle distorsioni risultanti, in questo caso in tubi portanti in acciaio. Un flusso a turbolenza k–∈ ed un modello di trasferimento di calore utilizzati hanno dimostrato di predire in modo sufficiente la distribuzione del coefficiente di trasferimento convettivo per numeri di Reynolds fino a circa $(0.3)10^6$.
A numeri di Reynolds superiori (qui sono stati analizzati fino a 10^6) riesce a fornire previsioni abbastanza valide nella maggior parte delle zone del cilindro sopravento e sottovento, e prevede bene gli angoli ai quali inizia la turbolenza e ai quali il flusso si separa, come pure l'esistenza di due valori massimi e due valori minimi nel coefficiente di trasferimento di calore. Tuttavia predice valori circa 100% più alti rispetto a quelli ottenuti attraverso i dati sperimentali disponibili nella zona di transizione laminare/turbolenza. Questo modello, come anche i dati sperimentali disponibili e i dati rappresentativi, sono stati utilizzati per definire la distribuzione del coefficiente di trasferimento di calore convettivo intorno alla superficie del pezzo come condizione limite di un programma agli elementi finiti sviluppato presso lo Swedish Institute for Metals Research realizzato per predire la storia della distribuzione di temperatura, trasformazioni di fase, distorsioni e proprietà meccaniche di pezzi in acciaio sottoposti a tempra.
Si è analizzata la dipendenza delle distorsioni dalla estensione della nonuniformità del coefficiente di trasferimento di calore convettivo.